Inorg. Chem. **2006**, *45*, 5585–5590

DFT Analysis of Co–Alkyl and Co–Adenosyl Vibrational Modes in B_{12}-Cofactors

Pawel M. Kozlowski,*,† Tadeusz Andruniow,†,‡ Andrzej A. Jarzecki,§ Marek Z. Zgierski,|| and Thomas G. Spiro⊥

Department of Chemistry, University of Louisville, Louisville, Kentucky 40292, Institute of Physical and Theoretical Chemistry, Department of Chemistry, Wroclaw University of Technology, 50-370 Wroclaw, Poland, Department of Chemistry, Brooklyn College and the Graduate School of the City University of New York, Brooklyn, New York 11230, Steacie Institute for Molecular Science, National Research Council of Canada, Ottawa, Ontario, Canada K1A OR6, Department of Chemistry, Princeton University, Princeton, New Jersey 08544

Received December 2, 2005

Density functional theory (DFT)-based normal mode calculations have been carried out on models for B_{12}-cofactors to assign reported isotope-edited resonance Raman spectra, which isolate vibrations of the organo–Co group. Interpretation is straightforward for alkyl–Co derivatives, which display prominent Co–C stretching vibrational bands. DFT correctly reproduces Co–C distances and frequencies for the methyl and ethyl derivatives. However, spectra are complex for adenosyl derivatives, due to mixing of Co–C stretching with a ribose deformation coordinate and to activation of modes involving Co–C–C bending and Co–adenosyl torsion. Despite this complexity, the computed spectra provide a satisfactory re-assignment of the experimental data. Reported trends in adenosyl–cobalamin spectra upon binding to the methylmalonyl CoA mutase enzyme, as well as on subsequent binding of substrates and inhibitors, provide support for an activation mechanism involving substrate-induced deformation of the adenosyl ligand.

Introduction

Nature exploits organometallic chemistry in the case of vitamin B_{12} by making and breaking cobalt−carbon bonds.[1−4] There are two B_{12} cofactors (Figure 1) in B_{12}-dependent enzymes, which support distinctive chemical pathways.[5] Enzymes utilizing methylcobalamin (MeCbl) catalyze methyl transfer reactions[6,7] in which the Co−C bond is cleaved heterolytically,[8] while enzymes employing adenosylcobalamin (AdoCbl) catalyze organic rearrangement reactions in which the first step is homolytic cleavage of the Co−C bond.[9−11] There is great interest in the mechanisms whereby

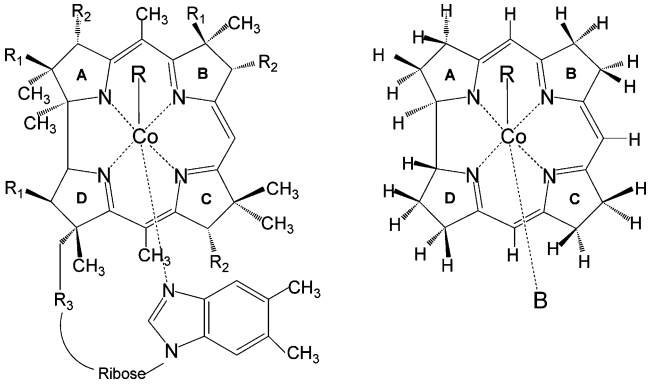

Figure 1. Molecular structure of B_{12} cofactors (left panel) where R = Me for MeCbl and R = Ado for AdoCbl (R_1 = CH_2CONH_2, R_2 = CH_2-CH_2CONH_2, R_3 = $(CH_2)_2CONHCH_2CH(CH_3)OPO_3$) Right panel: structural model of B_{12} cofactors employed in the present work, B−[Co^{III}corrin]−R^+ (B = DBI or Im, R = Me, Et, *iso*-Prop, or Ado).

* To whom correspondence should be addressed. Phone: (502) 852-6609. Fax: (502) 852-8149. E-mail: pawel@louisville.edu.
† University of Louisville.
‡ Wroclaw University of Technology.
§ Brooklyn College and the Graduate School of the City University of New York.
|| National Research Council of Canada.
⊥ Princeton University.

(1) *B_{12}*; Dolphin, D., Ed.; Wiley-Interscience: New York, 1982.
(2) Marzilli, L. G. In *Bioinorganic Catalysis*; Reedijk, J., Ed.; Marcel Dekker: New York, 1993; pp 227−259.
(3) *Vitamin B_{12} and B_{12} Proteins*; Kräutler, B., Arigoni, D., Golding, B. T., Eds.; Wiley-VCH: New York, 1998.
(4) Banerjee, R. *Chemistry and Biochemistry of B_{12}*; John Wiley and Sons: New York, 1999.
(5) Banerjee, R. *Chem. Biol.* **1997**, *4*, 175−186.
(6) Ludwig, M. L.; Matthews, R. G. *Annu. Rev. Biochem.* **1997**, *66*, 269−313.
(7) Mathews, R. G. *Acc. Chem. Res.* **2001**, *34*, 681−689.

10.1021/ic052069j CCC: $33.50
Published on Web 06/17/2006

the Co−C bond is activated toward heterolytic or homolytic cleavage in the B_{12}-dependent enzymes.

These processes can in principle be probed via vibrational spectroscopy.[12] Co−alkyl stretching vibrations have been detected by infrared and Raman spectroscopy,[13−16] and give an indirect indication of the Co−C bond strength.[17,18] Resonance Raman (RR) spectroscopy can provide access to B_{12}-containing proteins,[19−21] since laser tuning can be used to selectively excite cobalamin vibrations. Facile photolysis of Co−alkyl bonds is a significant hurdle, which can, however, be overcome cryogenically, since geminate recombination is efficient in frozen samples. Co−adenosyl vibrations have been detected in various functional states of the enzyme methylmalonylcoenzyme A mutase (MCM),[19,20] using $^{13/12}$C and CH/D isotope editing, and also in glutamate mutase (GLM).[21] The Co−methyl stretching vibration has been detected in a corrinoid/iron−sulfur protein.[22]

To interpret these spectroscopic signatures, one needs reliable assignments of the vibrational modes. The situation is straightforward in MeCbl, which gives a single strong Co−C stretching band at 506 cm^{-1},[12,14,18] but is not straightforward in AdoCbl, for which a number of features are seen in isotope difference RR spectra.[17−20] An assignment scheme was suggested,[18,20] based on physical arguments, and was used to infer a mechanism for activation by MCM[20] from changes in the spectral pattern when substrates and inhibitors were bound to the enzyme.

A primary motivation of the present work was to assess these assignments and interpretations using density functional theory (DFT) computation. DFT has been successful in modeling the geometries and spectroscopic properties including optical absorption, XES, or XPS and vibrational spectra of metal-containing compounds of considerable complexity, including metalloporphyrins[23,24] and cobalamins.[25−29] A previous vibrational study of a six-coordinate Im−[Co^{III}-corrin]−Me^+ model[30,31] permitted analysis of the most important interligand modes for MeCbl. The DFT-based force field accurately reproduced isotope shifts for interligand vibrations and provided a semiquantitative description of the corrin modes. Rovira et al.[32] have recently reported a computation of the full MeCbl structure, which produced an accurate Co−C stretching frequency (509 cm^{-1}). We now extend DFT to AdoCbl and find that the results require reassignment of the experimental spectra,[17−20] although the proposed activation mechanism in MCM is not substantially altered.

Methods

Calculations reported in this paper were carried out using gradient-corrected DFT with the Becke−Lee−Yang−Parr composite exchange correlation functional (B3LYP) as implemented in the Gaussian suite of programs for electronic structure calculations.[33] The B3LYP level of theory with 6-31G(d) [for H, C, and

(8) The heterolytic cleavage of the Co−C bond to form the methyl carbocation in cobalamin-dependent methyltransferases should not be taken literally: these heterolytic reactions are most likely nucleophilic displacement of S_N2-type, and the presence of free carbocations is not involved. Alternative mechanisms have been postulated for methyl transfer including oxidative addition and single electron transfer but are less probable (see ref 7 for details).

(9) Banerjee, R. *Biochem.* **2001**, *40*, 6191−6198.
(10) Toraya, T. *Chem. Rev.* **2003**, *103*, 2095−2127.
(11) Banerjee, R. *Chem. Rev.* **2003**, *103*, 2083−2094.
(12) Hirota, S.; Marzilli, L. G. Vibrational Spectroscopy of B_{12} and Related Compounds. In *Chemistry and Biochemistry of B_{12}*; Banerjee, R., Ed.; John Wiley and Sons, New York, 1999; Chapter 8.
(13) Ervin, A. M.; Shupack, S. I.; Byler. *Spectrosc. Lett.* **1984**, *17*, 603−613.
(14) Nie, S.; Marzilli, P. A.; Marzilli, L. G.; Yu, N.-T. *J. Chem. Soc., Chem. Commun.* **1990**, 770−771.
(15) Salama, S.; Spiro, T. G. *J. Raman Spectrosc.* **1977**, *6*, 57−60.
(16) Stich, T. R.; Brooks, A. J.; Buan, N. R.; Brunold, T. C. *J. Am. Chem. Soc.* **2003**, *125*, 5897−5914.
(17) Dong, S.; Padmakumar, R.; Banerjee, R.; Spiro, T. G. *J. Am. Chem. Soc.* **1996**, *118*, 9182−9183.
(18) Dong, S.; Padmakumar, R.; Banerjee, R.; Spiro, T. G. *Inorg. Chim. Acta.* **1998**, *270*, 392−398.
(19) Dong, S.; Padmakumar, R.; Maiti, N.; Banerjee, R.; Spiro, T. G. *J. Am. Chem. Soc.* **1998**, *120*, 9947−9948.
(20) Dong, S.; Padmakumar, R.; Banerjee, R.; Spiro, T. G. *J. Am. Chem. Soc.* **1999**, *121*, 7063−7070.
(21) Huhta, M. S.; Chen, H.-P.; Hemann, C.; Hille, C. R.; Marsh, E. N. G. *Biochem. J.* **2001**, *355*, 131−137.
(22) Stich, T. A., Seravalli, J., Venkateshrao, S., Spiro, T. G., Ragsdale, S. W., Brunold, T. C. *J. Am. Chem. Soc.* **2006**, *128*, 5010−5020.
(23) Ghosh, A. *Acc. Chem. Res.* **1998**, *31*, 189−198. Ghosh, A. Quantum Chemical Studies of Molecular Structures and Potential Energy Surfaces of Porphyrins and Hemes. In *The Porphyrin Handbook*; Kadish, K. M., Guilard, R., Smith, K. M., Eds.; Academic Press: New York, 1999; Vol. 7, pp 1−38.
(24) Spiro, T. G.; Kozlowski, P. M.; Zgierski, M. Z. *J. Raman Spectrosc.* **1998**, *29*, 869−879. Spiro, T. G.; Zgierski, M. Z.; Kozlowski, P. M. *Coord. Chem. Rev.* **2001**, *219−221*, 923−936.
(25) Andruniow, T.; Zgierski, M. Z.; Kozlowski, P. M. *Chem. Phys. Lett.* **2000**, *331*, 509−515. Andruniow, T.; Zgierski, M. Z.; Kozlowski, P. M. *J. Phys. Chem. B* **2000**, *104*, 10921−10927. Andruniow, T.; Zgierski, M. Z.; Kozlowski, P. M. *J. Am. Chem. Soc.* **2001**, *123*, 2679−2680. Kozlowski, P. M. *Curr. Opin. Chem. Biol.* **2001**, *5*, 736−743. Kozlowski, P. M.; Zgierski, M. Z. *J. Phys. Chem. B* **2004**, *108*, 14163−14170.
(26) Jensen, K. P., Ryde, U. *J. Mol. Struct. (THEOCHEM)* **2002**, *585*, 239−255. Jensen, K. P.; Ryde, U. *J. Am. Chem. Soc.* **2003**, *125*, 13970−13971.
(27) Dölker, N.; Maseras, F.; Llenos, A. *J. Phys. Chem. B* **2001**, *105*, 7564−7571. Dölker, N.; Maseras, F.; Lledos, A. *J. Phys. Chem. B* **2003**, *107*, 306−315. Dölker, N.; Maseras, F.; Siegbahn, P. E. M. *Chem. Phys. Lett.* **2004**, *386*, 174−178. Dölker, N.; Morreale, A.; Maseras, F. *J. Biol. Inorg. Chem.* **2005**, *10*, 509−517.
(28) Ouyang, L.; Randaccio, L.; Rulis, P.; Kurmaev, E. Z.; Moewes, A.; Ching, W. Y. *J. Mol. Struct. (THEOCHEM)* **2003**, *622*, 221−227. Kurmaev, E. Z.; Moewes, A.; Ouyang, L.; Randaccio, L.; Rulis, P.; Ching, W.-Y.; Bach, M.; Neumann, M. *Europhys. Lett.* **2003**, *62*, 582−587. Ouyang, L.; Rulis, P.; Ching, W.-Y.; Slouf, M.; Nardin, G.; Randaccio, L. *Spectochim. Acta A* **2005**, *61*, 1647−1652.
(29) Ouyang, L.; Rulis, P.; Ching, W. Y.; Nardin, G.; Randaccio, L. *Inorg. Chem.* **2004**, *43*, 1235−1241.
(30) Andruniow, T.; Zgierski, M. Z.; Kozlowski, P. M. *Chem. Phys. Lett.* **2000**, *331*, 502−508.
(31) Andruniow, T.; Zgierski, M. Z.; Kozlowski, P. M. *J. Phys. Chem. A* **2002**, *106*, 1365−1373.
(32) Rovira, C.; Biarnes, X.; Kunc, K. *Inorg. Chem.* **2004**, *43*, 6628−6632.
(33) Frisch, M. J.; Trucks, G. W.; Schlegel, H. B.; Scuseria, G. E.; Robb, M. A.; Cheeseman, J. R.; Montgomery, J. A., Jr.; Vreven, T.; Kudin, K. N.; Burant, J. C.; Millam, J. M.; Iyengar, S. S.; Tomasi, J.; Barone, V.; Mennucci, B.; Cossi, M.; Scalmani, G.; Rega, N.; Petersson, G. A.; Nakatsuji, H.; Hada, M.; Ehara, M.; Toyota, K.; Fukuda, R.; Hasegawa, J.; Ishida, M.; Nakajima, T.; Honda, Y.; Kitao, O.; Nakai, H.; Klene, M.; Li, X.; Knox, J. E.; Hratchian, H. P.; Cross, J. B.; Bakken, V.; Adamo, C.; Jaramillo, J.; Gomperts, R.; Stratmann, R. E.; Yazyev, O.; Austin, A. J.; Cammi, R.; Pomelli, C.; Ochterski, J. W.; Ayala, P. Y.; Morokuma, K.; Voth, G. A.; Salvador, P.; Dannenberg, J. J.; Zakrzewski, V. G.; Dapprich, S.; Daniels, A. D.; Strain, M. C.; Farkas, O.; Malick, D. K.; Rabuck, A. D.; Raghavachari, K.; Foresman, J. B.; Ortiz, J. V.; Cui, Q.; Baboul, A. G.; Clifford, S.; Cioslowski, J.; Stefanov, B. B.; Liu, G.; Liashenko, A.; Piskorz, P.; Komaromi, I.; Martin, R. L.; Fox, D. J.; Keith, T.; Al-Laham, M. A.; Peng, C. Y.; Nanayakkara, A.; Challacombe, M.; Gill, P. M. W.; Johnson, B.; Chen, W.; Wong, M. W.; Gonzalez, C.; Pople, J. A. *Gaussian 03*, revision C.02; Gaussian, Inc.: Wallingford, CT, 2004.

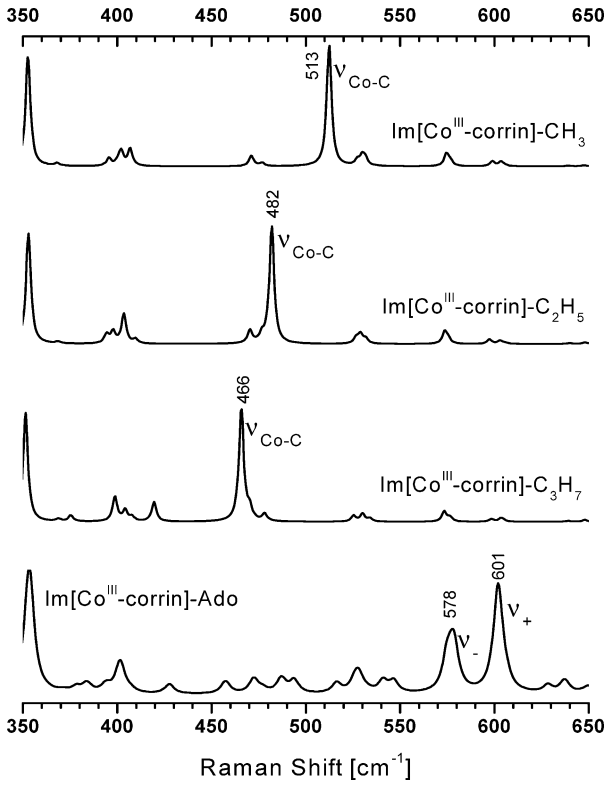

Figure 2. Simulated nonresonance Raman spectra, in the low-frequency region, for the indicated Im−[Co^{III}corrin]−R$^+$ models (R = Me, Et, *iso*-Prop, and Ado). A uniform scaling factor (0.86) was applied to B3LYP force constants for all shown models.

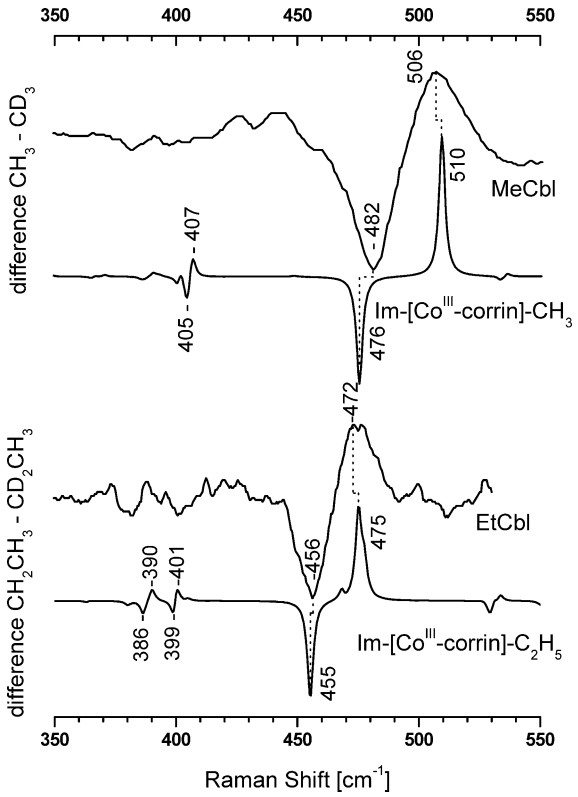

Figure 3. Comparison of computed isotope difference spectra for Im−[Co^{III}corrin]−R$^+$ (R = Me and Et) with experimental spectra (ref 18) for MeCbl and EtCbl. Computed spectra are based on refined B3LYP force constants applying multiple scaling factors. The alignment of experimental spectra to one common scale might be slightly affected by electronic manipulation of digitalized data.

N atoms] and Ahlrichs VTZ (for Co) basis sets, successfully used in previous calculations on cobalamins, was employed in the present study. Frequency calculation and nonresonance Raman intensities based upon polarizability derivatives have been carried for all the B−[Co^{III}corrin]−R$^+$ structural models (Figure 1). Cartesian force constants calculated at the optimized geometry were transformed to natural internal coordinates.[34] These coordinates were generated by the FCT (Force Constant Transformation) program, which is included in TX90 program package[35] and manually augmented. To refine the calculated DFT force constants, we employed the SQM procedure, which scales the original DFT force constants according to the formula $F_{ij}' = (\lambda_i\lambda_j)^{1/2}F_{ij}$. The SQM procedure allows application of single or multiscale factors to refine the originally computed force constants and to obtain scaled frequencies and their refined vibrational modes. Our vibrational analysis was performed with the following strategy. First, the SQM refinement of force constants was utilized with a single scaling factor ($\lambda = 0.86$)[31] for all computed models of Im−[Co^{III}corrin]−R$^+$ (R = Me, Et, *iso*-Prop, and Ado). Resulting nonresoonance Raman spectra are shown in Figure 2. For a final comparison of computed isotope difference spectra for Im−[Co^{III}corrin]−R$^+$ (R = Me, Et, and Ado) with experimental spectra, we have decided to refine the originally computed force constants using the SQM set of seven scaling factors. This SQM set of scaling factors has been shown previously to produce very reliable frequencies, especially for porphyrin-based structures.[36] The computed isotope difference spectra of Im−[Co^{III}-corrin]−R$^+$ (R = Me, Et, and Ado) are compared with experimental spectra in Figures 3 and 4.

Results and Discussion

Alkyl Corrins. As in previous studies,[25−27] DFT gives satisfactory geometries for alkyl corrins (Table 1). For the methyl adduct, the Co−C distance is short, 1.96 Å, as it is in MeCbl (1.98 Å)[37] while the bond to the axial imidazole is long, 2.22 Å, as is the Co−dimethylbenzimidazole bond in MeCbl (2.16 Å).[37] Changing the alkyl group to ethyl lengthens the Co−C bond, to 1.99 Å, due to a combination of electronic and nonbonded ethyl−corrin interactions, while increasing the steric bulk further, to propyl, lengthens the Co−C bond to 2.03 Å. Interestingly, the Co−imidazole bond lengthens in the same order, to 2.26 and 2.32 Å, illustrating what has become known as the 'inverse trans influence'.[38−43]

(34) Fogarasi, G.; Zhou, X.; Taylor, R. W.; Pulay, P. *J. Am. Chem. Soc.* **1992**, *114*, 8191−8201.
(35) Pulay, P. *TX90*; Fayetteville, AR, 1990. Pulay, P. *Theor. Chim. Acta* **1979**, *50*, 229.
(36) An original set of six scaling factors previously optimized and extensively applied to metalloporphyrins (see for example Stoll, L. K.; Zgierski, M. Z.; Kozlowski, P. M. *J. Phys. Chem. A* **2003**, *107*, 4165−4171) was augmented by one extra scaling factor (0.74) applied to Co−C stretching mode of the cofactor model.
(37) Randaccio, L.; Furlan, M.; Geremia, S.; Slouf, M.; Srnova, I.; Toffoli, D. *Inorg. Chem.* **2000**, *39*, 3403−3413.
(38) Bresciani-Pahor, N.; Forcolin, M.; Marzilli, L. G.; Randaccio, L.; Summers, M. F.; Toscano, P. J. *Coord. Chem. Rev.* **1985**, *63*, 1−125.
(39) Randaccio, L.; Bresciani-Pahor, N.; Zangrando, E.; Marzilli, L. G. *Chem. Soc. Rev.* **1989**, *18*, 225−250.
(40) De Ridder, D. J. A.; Zangrando, E.; Bürgi, H.-B. *J. Mol. Struct.* **1996**, *374*, 63−83.
(41) Randaccio, L. *Comments Inorg. Chem.* **1999**, *21*, 327−376.
(42) Randaccio, L.; Geremia, S.; Stener, M.; Toffoli, D.; Sangrando, E. *Eur. J. Inorg. Chem.* **2002**, 93−103.
(43) Andruniow, T.; Zgierski, M. Z.; Kozlowski, P. M. *Chem. Phys. Lett.* **2005**, *410*, 410−416.

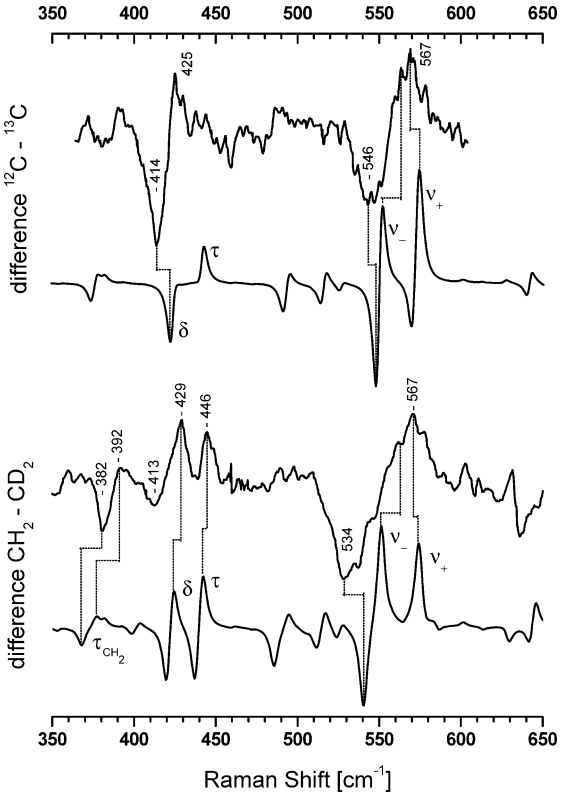

Figure 4. Comparison of computed isotope difference spectra for Im−[Co^{III}corrin]−Ado^+, with experimental spectra (ref 20 for AdoCbl). Computed spectra are based on refined B3LYP force constants applying multiple scaling factors and empirical enhancement of Raman intensities for δ and τ modes (see text for details). The alignment of experimental spectra to one common scale might slightly be affected by electronic manipulation of digitalized data.

Table 1. R−CoCbl Bond Lengths (Å), Force Constants (mdyn/Å), Stretching Frequencies, and Isotope Shifts (cm^{-1})

	calcd Co−C		calcd ν_{Co-C}			exptl ν_{Co-C}		
	length	force conts.	ν_{Co-C}	$\Delta(D)$	$\Delta(^{13}C)$	ν_{Co-C}	$\Delta(D)$	$\Delta(^{13}C)$
Me−	1.962	4.824	510	32	12	506	24	13
Et−	1.989	2.145	475	20	10	472	12	
iso-Prop−	2.033	2.002	466	10	8			

[a] $\Delta(D)$: CH_2/CD_2 shift for the CH_2 bounded to Co. [b] $\Delta(^{13}C)$: $^{12}CH_2/^{13}CH_2$ shift for the C atom bounded to Co.

The computed frequencies fall in the same order, as expected. The Co−C stretching frequencies are in excellent agreement with reported values for MeCbl and EtCbl; no data are available for isopropyl derivatives. Stretching frequencies for the axial base have not been reported; searches of the Me−cobinamide RR spectrum using isotopically labeled imidazole as axial base have been unsuccessful, presumably due to inadequate resonance enhancement.[44] The computed Co-imidizole stretches are at very low frequencies (~100 cm^{-1})[30,31] reflecting the very weak bonds. Interestingly, Rovira et al.[32] computed a much higher frequency for the Co-dimethylbenzimidazole stretch in MeCbl, 437 cm^{-1}, consistent with a somewhat shorter Co−N bond, 2.15 Å; possibly the covalent attachment of the dimethylbenzimidazole ligand to the corrin ring produces this shortening, via the chelate effect.

(44) Cwickel, D.; Spiro, T. G. unpublished results.

Figure 2 shows computed Raman spectra for the alkylcorrin-imidazole complexes in the low-frequency region. Most of the bands arise from corrin vibrations, but the Co−C stretches stand out strongly. The computed intensities are based on classical polarizability derivatives and do no capture selective resonance effects. Nevertheless the Co−C stretches show up prominently in RR spectra of MeCbl and EtCbl. Figure 3 shows an excellent match of the observed $^{13/12}C$ and CH/D difference spectra with computed ones for the corrin−imidazole analogues. On the other hand, the computed Co−imidazole bands are very weak and it is not surprising that the analogous cobalamin bands have not been detected.

Adenosyl Corrins. Computed Co−C and Co−imidazole bond distances for Im-[Co^{III}corrin]-Ado^+, 1.99 and 2.22 Å, are similar to those of the ethyl adduct (Table 1) and are in satisfactory agreement with the corresponding distances, 2.033 and 2.237 Å, in AdoCbl.[29] The DFT calculations employing the B3LYP functional do not capture the trend which is experimentally observed for axial bond distances in AdoCbl[29] and MeCbl[37] cofactors. This most likely reflects structural simplifications introduced by truncating the AdoCbl side chains and replacing the dimethylbenzimidazole ligand with imidazole. Furthermore, the hybrid B3LYP functional does not perform as well as nonhybrid BP86, as has been recently demonstrated.[45,46] For both functionals, the frequencies for the Co−C bond stretch are overestimated and the force constants have to be scaled in order to obtain reasonable agreement with experiment. While the BP86 value is closer to experiment, the overall performance from a statistical point of view is better for B3LYP. Consequently, the latter was used in recent DFT analyses of Co−alkyl and Co−adenosyl vibrational modes in B_{12}-cofactors, consistent with previous studies.[30,31]

The computed Raman spectrum (Figure 2) is very complex; no dominant Co−C stretching band can be seen. Figure 4 shows the experimental $^{13/12}C$ and CH/D difference spectra for AdoCbl, reported by Dong et al.,[20] and compares them with the DFT-computed difference spectra. (The intensities of the bands marked δ and τ were enhanced for visualization. Although their computed polarizability derivatives are low, they may be enhanced resonantly if the excited state is displaced along their normal coordinates. They are both polarized and are subject to the dominant Franck−Condon enhancement mechanism.) Difference spectroscopy was used in order to cancel out the numerous RR contributions from corrin modes and to isolate those vibrations associated with the Co−Ado unit. It was recognized that the complex spectral pattern required at least four isotope-sensitive vibrations, and these were proposed to be Co−C stretching (430 cm^{-1}), ribose ring deformation (569 cm^{-1}), Co−C−C bending (363 cm^{-1}), and a torsion of the adenosyl ligand about the Co−C bond (420 cm^{-1}). Indeed, the computed difference spectra reveal four bands with the requisite isotope sensitivity.

Band shapes in the difference spectra are functions of the intensities, widths, and isotope shifts of the parent bands, and since the computed intensities do not take resonance enhancement into account, the computed difference spectrum

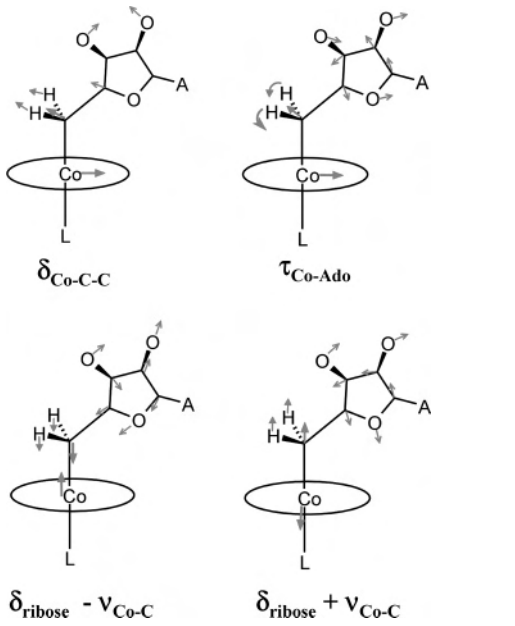

Figure 5. Schematic eigenvectors for the four isotope-sensitive Co−Ado modes identified in Figure 4.

cannot be expected to reproduce the experimental one faithfully. Nevertheless, there is a reasonable correspondence between the experimental difference bands and the main features of the computed spectra. The broad sigmoidal feature at 567/546 cm^{-1} in the $^{13/12}C$ difference spectrum and at 567/534 cm^{-1} in the CH/D difference spectrum coincides with two computed modes having differing isotope sensitivities; the apparently greater CH/D isotope shift can be accounted for by the stronger negative peak computed at 540 cm^{-1} in the CH/D difference spectrum. Experimental $^{13/12}C$ and CH/D difference spectra each show a 425 cm^{-1} band, which finds a prominent corresponding band in the computed spectra, while computed and experimental spectra both show a neighboring 446 cm^{-1} band only in the CH/D difference spectra. Finally, there is a weak computed couplet corresponding to the 392/382 cm^{-1} couplet seen in the CH/D experimental spectrum. As might be expected, there are additional minor bands in the computed difference spectra which are not observed in the experimental spectra, presumably because of weak resonance enhancement.

The eigenvectors of the four most prominent modes are illustrated in Figure 5. They involve the same vibrational coordinates, as had been inferred from the experimental spectra, namely Co−C stretching and torsion, Co−C−C bending, and ribose deformation. However, the computations show the Co−C stretching coordinate to be heavily mixed with ribose deformation, giving rise to the two modes near 560 cm^{-1}. The coordinates combine in phase for the higher-frequency mode, labeled $\delta_R + \nu_{CoC}$, and out of phase for the-lower frequency mode, $\delta_R - \nu_{CoC}$. As a result, there is no 'Co−C stretch' in the expected 400−500 cm^{-1} region as there is for the simpler alkyl corrins. The previous attribution of the 425 cm^{-1} band to Co−C stretching was based on a reduced-mass model for the Ado ligand. This model is adequate for the alkyl cobalamins but fails for AdoCbl because of the kinematic effect of the ribose ring, whose deformation coordinate interacts strongly with the Co−C displacement.

Table 2. Isotope-Sensitive AdoCbl Modes (cm^{-1})

calculated			experimental			
ν	$\Delta(D)$	$\Delta(^{13}C)$	ν	$\Delta(D)$	$\Delta(^{13}C)$	mode character
574	34	4	567			$\nu_{Co-C} + \delta_{ribose}$
550	10	3				$\nu_{Co-C} - \delta_{ribose}$
441	6	2	446			τ_{Co-Ado}
424	6	2	429	16	11	δ_{Co-C-C}
376	11	3	392	10		$\tau-CH_2$

Instead, the 425 cm^{-1} mode is seen (Figure 5) to be Co−C−C bending in character (δ_{CoCC}); its relatively high frequency reflects the steric crowding of the Ado ligand with the corrin ring. The 440 and 380 cm^{-1} modes both involve torsional motions about the Co−C bonds. The H atoms of the $Co-CH_2$ group undergo significant motion, while the C atom does not; this is why the bands are seen in the CH/D difference spectrum but not in the $^{13/12}C$ difference spectrum. The higher-frequency torsion mode has significant contribution from Co−N(corrin) bond stretching ($\tau_{CoC} + \nu_{CoN}$), while the lower-frequency mode (τ'_{CoC}) does not (Table 2). Even the lower of these modes, 380 cm^{-1}, is much higher than would be expected for simple torsion about a single bond and again reflects the nonbonded interactions of the Ado ligand with the corrin ring.

Implications for Protein Activation of B_{12} Coenzymes. Despite the reassignments required by the DFT-based normal mode analysis, the inferences about enzyme activation of AdoCbl which were drawn from the RR study of MCM are still supported. In that study, isotope difference spectra were monitored as the coenzyme was bound to the apoenzyme, and then substrates or inhibitors were added. For all these samples, the 567 cm^{-1} band appeared at the same frequency, though with somewhat variable relative intensity. The identification of this broad band as $\delta_R + \nu_{CoC}$ plus $\delta_R - \nu_{CoC}$ implies that the Co−C bond strength is unaffected by interaction of the cofactor with the enzyme or the subsequent binding of substrates or inhibitors. This finding is also supported by recent QM/MM calculations which show that in the case of MCM the Co−C bond remains intact upon coenzyme binding to apoenzyme.[47] There is no indication that the activation mechanism involves Co−C bond weakening.

However, there are RR spectral changes in the 350−450 cm^{-1} region, which, in light of the current assignments, imply that the Co−C−C bending and Co−C torsion coordinates are affected. Specifically, the intensity is diminished for δ_{CoCC}, but augmented for τ'_{CoC}, as coenzyme binds to the enzyme, and these trends are accentuated when substrate is bound to the active site. These changes in resonance enhancement imply diminished and augmented displacements along the δ_{CoCC} and τ'_{CoC} coordinates between the ground and the resonant excited state of the chromophore. The

(45) Jensen, K. P.; Ryde, U. *J. Phys. Chem. A* **2003**, *107*, 7539−7545.
(46) Kuta, J.; Patchkovskii, S.; Zgierski, M. Z.; Kozlowski, P. M. *J. Compt. Chem.* **2006**, *27*, in press.
(47) Freindorf, M., Kozlowski, P. M. *J. Am. Chem. Soc.* **2004**, *126*, 1928−1929.

altered displacements in turn imply bending and twisting of the Ado ligand in either the ground or the excited states, or both.

These kinds of ligand distortions have become the favored explanation for enzymatic activation of AdoCbl[10,11] since alternative effects, including modulation of the trans ligand bond, or distortions of the corrin ring have been largely ruled out. Recent crystallographic studies for two B_{12}-containg enzymes, glutamate mutase (GLM)[48] and diol dehydratase (DDH),[49] suggest that the main contribution to Co−C bond cleavage is substrate-induced deformation of the coenzyme, although the evidence is complicated by the likelihood that the Co(III) is reduced to Co(II) in the crystals. Recent QM/MM calculations reported by Jensen and Ryde[50] likewise support adenosyl deformation as the most feasible mechanism of Co−C activation.

One can speculate that nature has chosen the complex Ado ligand because it offers a ready handle for substrate-induced deformation. The misalignment of the bonding orbitals resulting from such deformations weaken the Co−C bond along the homolytic dissociation coordinate. In contrast, the small methyl ligand does not facilitate substrate-induced deformation and MeCbl enzymes do not promote Co−C homolysis. Instead, they facilitate heterolytic cleavage by promoting electrophilic diplacement of the methyl cation.

IC052069J

(48) Gruber, K.; Reitzer, R.; Kratky, C. *Angew. Chem., Int. Ed.* **2001**, *40*, 3377−3380.
(49) Shibata, N.; Masuda, J.; Morimoto, Y.; Yasuoka, N.; Toraya, T. *Biochemistry* **2002**, *41*, 12607−12617.
(50) Jensen, K. P.; Ryde, U. *J. Am. Chem. Soc.* **2005**, *127*, 9117−9128.